

# Solubilities of Cerium(IV), Terbium(III), and Iron(III) $\beta$ -Diketonates in Supercritical Carbon Dioxide<sup>†</sup>

Wendy C. Andersen,<sup>‡,§</sup> Robert E. Sievers,<sup>\*,§</sup> Anthony F. Lagalante,<sup>‡</sup> and Thomas J. Bruno<sup>‡</sup>

Chemical Science and Technology Laboratory, National Institute of Standards and Technology, 325 Broadway, Boulder, Colorado 80305, and Department of Chemistry and Biochemistry, University of Colorado, Boulder, Colorado 80309

The solubilities of the cerium(IV), terbium(III), and iron(III) chelates of the anions of 2,2,7-trimethyl-3,5-octanedionate, H(tod), 2,2,6,6-tetramethyl-3,5-octanedionate, H(thd), and 2,4-pentanedionate, H(acac), were measured in supercritical carbon dioxide by near-infrared spectroscopy from 313 to 333 K and 10 to 35 MPa with a high-pressure optical cell. Solubilities increased in the order acac < thd < tod for all metal  $\beta$ -diketonates, with Ce(tod)<sub>4</sub>, Tb(tod)<sub>3</sub>, and Fe(tod)<sub>3</sub> an order of magnitude more soluble than Ce(thd)<sub>4</sub>, Tb(thd)<sub>3</sub>, and Fe(acac)<sub>3</sub>, respectively. For the larger metal ions, Ce<sup>4+</sup> and Tb<sup>3+</sup>, the flexibility of the isobutyl group in the tod ligand creates a more lipophilic shell around the central metal ion, increasing the solubility of the chelate in CO<sub>2</sub>. These observations indicate that the isobutyl group is at least as CO<sub>2</sub>-philic as the *tert*-butyl moiety. The experimental solubilities were correlated using the model proposed by Chrastil.

## Introduction

Supercritical fluid extraction (SFE) with carbon dioxide has been proposed as an environmentally benign extraction process for analytical- to industrial-scale separations in fields as varied as environmental analysis and consumer product processing. The use of supercritical CO<sub>2</sub> containing chelating agents is an attractive technique for the remediation of metal-contaminated wastes or the extraction of high-value metals because the metal is both removed and concentrated in the precipitated extract, eliminating the need for additional concentration steps.  $\beta$ -Diketone ligands form a lipophilic shell around metal ions, enabling the dissolution of the metal chelate in nonpolar supercritical CO<sub>2</sub>. As a result, these chelating agents have been widely used to extract metal ions from a variety of sample matrices using SFE.<sup>1–3</sup> For metal extraction, accurate solubility data for the metal  $\beta$ -diketonate complex in CO<sub>2</sub> are crucial for designing efficient SFE methods. While the solubilities of many metal chelates have been measured in supercritical CO<sub>2</sub>,<sup>4,5</sup> some of the most promising and inexpensive chelates have not yet been studied.

In the current study, the solubilities of cerium(IV), terbium(III), and iron(III)  $\beta$ -diketonate complexes with the ligands 2,2,7-trimethyl-3,5-octanedione, H(tod), 2,2,6,6-tetramethyl-3,5-heptanedione, H(thd), and 2,4-pentanedione, H(acac), were determined. The solubilities were measured spectroscopically in supercritical CO<sub>2</sub> from 313 to 333 K and from 10 to 35 MPa by a static near-infrared (NIR) method. NIR is particularly well suited for measuring the absorbance of highly colored (or colorless) metal chelates that have prohibitively high (or low) absorptivities in the ultraviolet and visible regions. In addition, molar absorp-

tivities in the NIR do not show a strong dependence on the density of the supercritical fluid, as is the case in the UV–visible spectra.<sup>6</sup> The solubility data were interpreted with respect to the structure of these metal chelates and correlated with the empirical model proposed by Chrastil.<sup>7</sup> All data reported herein include a combined standard uncertainty based on one standard deviation of the measurement result.<sup>8</sup>

## Experimental Section

**Chemicals.** SFC grade carbon dioxide was used as received from a commercial supplier. Ce(thd)<sub>4</sub>, Tb<sub>2</sub>(thd)<sub>6</sub>, Fe(thd)<sub>3</sub>, and Fe(acac)<sub>3</sub> were purchased from commercial suppliers. All chemicals were used as received; however, disparate solubility results were initially found for Tb<sub>2</sub>(thd)<sub>6</sub> and Fe(thd)<sub>3</sub> and led us to further purify these compounds by heating for 2 h under vacuum (388 and 353 K, respectively) to remove a possible free ligand impurity. Ce(tod)<sub>4</sub>, Tb<sub>2</sub>(tod)<sub>6</sub>, Fe(tod)<sub>3</sub>, and H(tod) were synthesized and purified according to methods in the literature.<sup>9,10</sup> Although solid Tb<sub>2</sub>(tod)<sub>6</sub> and Tb<sub>2</sub>(thd)<sub>6</sub> are dimeric, the monomers are obtained by dissolution in organic solvents.<sup>9</sup>

**Solubility Apparatus.** The solubility measurement apparatus consisted of a high-pressure syringe pump, an NIR spectrophotometer, an optical cell with a thermostat, and a pressure transducer (Figure 1). A commercial scanning UV–visible–NIR spectrophotometer was used for all experiments, set for 4.0 nm resolution and a scan speed of 2000 nm/min. The optical cell was custom built from 316 stainless steel and was fitted with sapphire windows (0.64 cm thick) sealed with polyetheretherketone (PEEK) gaskets. A cavity at the bottom of the cell accommodated a Teflon-coated magnetic stirring bar, coupled to an external magnetic stirring device. The cell had a path length of 3.93 ± 0.06 cm and an internal volume of 2.80 ± 0.01 mL. The entire cell was thermostated in an aluminum block by four cartridge heaters. A platinum resistance temperature sensor was used to measure and control the temperature

<sup>†</sup> This contribution will be part of a special print edition containing papers presented at the Fourteenth Symposium on Thermophysical Properties, Boulder, CO, June 25–30, 2000.

\* To whom correspondence should be addressed. Fax: (303) 492-1414. E-mail: rosella@terra.colorado.edu.

<sup>‡</sup> National Institute of Standards and Technology.

<sup>§</sup> University of Colorado, Boulder.

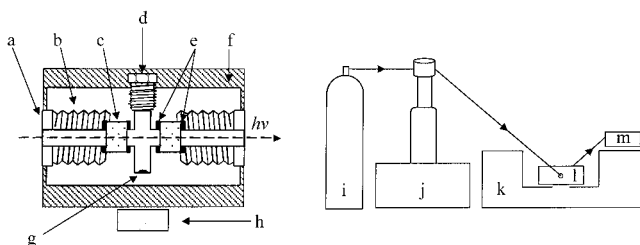


**Figure 1.** High-pressure near-infrared cell (left) and experimental setup (right): (a) end fitting; (b) cell body; (c) sapphire window; (d) sample inlet port; (e) PEEK gaskets; (f) thermostat; (g) stir bar; (h) magnetic stirrer; (i) CO<sub>2</sub> cylinder; (j) high-pressure syringe pump; (k) near-infrared spectrophotometer; (l) cell; (m) pressure transducer.

**Table 1. Molar Absorptivity and Absorbance Maxima of Metal Chelates in Supercritical CO<sub>2</sub>**

metal chelate	$\epsilon/\text{L}\cdot\text{mol}^{-1}\cdot\text{cm}^{-1}$	$\lambda_{\text{max}}/\text{nm}$
Ce(tod) <sub>4</sub>	2.43 ± 0.07	1696
Tb(tod) <sub>3</sub>	1.67 ± 0.03	1696
Fe(tod) <sub>3</sub>	1.73 ± 0.03	1696
Ce(thd) <sub>4</sub>	19.0 ± 1.8	2308
Tb(thd) <sub>3</sub>	6.71 ± 0.14	2306
Fe(thd) <sub>3</sub>	1.97 ± 0.03	1694
Fe(acac) <sub>3</sub>	4.09 ± 0.12	2264

to within ±0.1 K using a microprocessor-based temperature controller. The cell pressure was monitored in-situ to within ±1% by a pressure transducer calibrated using a dead weight pressure balance primary standard.

**Solubility Measurement.** The solute was loaded into a basket made of stainless-steel mesh, and was placed into the cell above the optical path. The cell was then purged with CO<sub>2</sub> to remove air, and sealed. The system was heated to the desired temperature and pressurized with CO<sub>2</sub> from a syringe pump, and the solution was allowed to equilibrate while being stirred. The cell was pressurized in 1 to 3 MPa increments over the range 10 to 25 MPa, with absorbance measurements made after attaining equilibrium at each pressure. Equilibration times were typically 15 to 30 min, although Tb(thd)<sub>3</sub> and Fe(thd)<sub>3</sub> required up to 1 h to equilibrate. After constant absorbance was attained, spectra were measured in triplicate from 1300 to 2500 nm. At all pressures, the background absorbance from CO<sub>2</sub> in the quantitative region was less than the standard deviation of replicate measurements. Therefore, no background corrections were necessary.

**Calibration.** All calibration standards were prepared by adding a known amount of the metal chelate to the cell, heating the cell, and pressurizing the contents with CO<sub>2</sub> until the absorbance of the peak maximum ( $\lambda_{\text{max}}$ ) remained constant with the addition of CO<sub>2</sub>. The absorbance was calculated by subtracting the baseline absorbance value at 1518 nm from the absorbance at  $\lambda_{\text{max}}$  (Table 1). Each standard was measured in triplicate, and Beer–Lambert law plots were attained with correlation coefficients ( $R^2$ ) of 0.9970 to 0.9998.

## Results and Discussion

**Solubility Measurement.** The concentration of a given metal chelate in supercritical CO<sub>2</sub> was determined using the Beer–Lambert law. Two NIR regions were available for analysis: the first overtone region of the C–H stretching vibration (1650 to 1800 nm) and the more intense combination band region (2250 to 2500 nm). We used the overtone region to quantify the solubility of the more soluble chelates, and the combination region for the less soluble chelates.

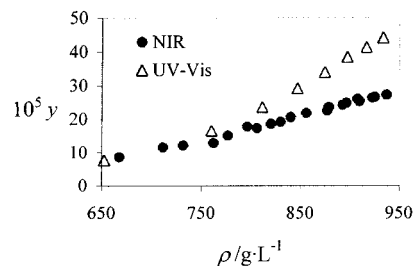


**Figure 2.** Solubility of Fe(acac)<sub>3</sub> in supercritical carbon dioxide at 313 K determined by NIR and UV–visible static methods.

Molar absorptivity coefficients,  $\epsilon$ , for the metal chelates are listed in Table 1. For hydrocarbons,  $\epsilon$  has been shown to be pressure dependent in UV–visible and IR spectroscopy,<sup>6,11</sup> however, others have found very little change in  $\epsilon$  with increasing pressure or temperature using NIR spectroscopy.<sup>12</sup> We also found  $\epsilon$  to be independent of pressure and temperature for the chelates studied. Nine replicate measurements of  $\epsilon$  for five different concentrations of Ce(tod)<sub>4</sub> at 323 and 333 K gave an average relative standard deviation of 0.9% over the pressure range 16.2 to 32.2 MPa. Moreover, we did not observe a shift in  $\lambda_{\text{max}}$  over the range of these measurements.

While several researchers have used NIR to determine the solubility of organic compounds in supercritical fluids, this is the first study of metal chelate solubility by NIR. To check the accuracy of the NIR static method, the solubility of Fe(acac)<sub>3</sub> was measured in CO<sub>2</sub> and compared to the Fe(acac)<sub>3</sub> solubility isotherm at 313 K obtained by Lagalante<sup>13</sup> using a UV–visible static method.<sup>14</sup> The two data sets are shown in Figure 2. There is good agreement between the two data sets at lower densities; however, at the highest density measured, the UV–visible solubility is 1.6 times higher than the NIR one. As the UV–visible data were calibrated to liquid solvent standards, the differences between these data sets fall within the range observed by Rice.<sup>6</sup> The reproducibility of two replicate NIR measurements for Fe(acac)<sub>3</sub> at 313 K was ±1.8%, comparable to the experimental uncertainty of the UV–visible method (±2.0%).

Tables 2–5 summarize the measured solubilities of the complexes in mole fraction,  $y$ , and solubility,  $S$  (g/L), as a function of CO<sub>2</sub> density. In these experiments, the density was calculated at the experimental temperature and pressure of pure CO<sub>2</sub>.<sup>15</sup> For the more soluble chelates, however, the large quantity of solute dissolved in CO<sub>2</sub> is expected to cause a discrepancy between the actual and calculated densities. Solubility data are expressed with an average relative standard deviation of 4.6% based on two to three separate measurements of the 313, 323, and 333 K isotherms of Tb(tod)<sub>3</sub>. Compared with literature solubility data,<sup>4,5</sup> Ce(tod)<sub>4</sub>, Tb(tod)<sub>3</sub>, Fe(tod)<sub>3</sub>, and Fe(thd)<sub>3</sub> are among the most soluble metal chelates studied to date, including the CO<sub>2</sub>-philic fluorinated metal chelates.

Ce(tod)<sub>4</sub> and Tb(tod)<sub>3</sub> are an order of magnitude more soluble than Ce(thd)<sub>4</sub> and Tb(thd)<sub>3</sub>. We have recently determined the crystal structures of the tod chelates and found that tod forms a more compact ligand shell around Ce<sup>4+</sup> and Tb<sup>3+</sup> than does thd.<sup>9</sup> Although tod and thd are isomers, thd is sterically rigid, while the isobutyl group of tod is more flexible. Better shielding of the highly charged Ce<sup>4+</sup> and Tb<sup>3+</sup> by tod increases the lipophilicity and solubility of the tod chelates in nonpolar supercritical CO<sub>2</sub>. These measurements indicate that  $\beta$ -diketonates containing isobutyl groups can be more CO<sub>2</sub>-philic than those with *tert*-butyl groups in facilitating solubility in supercritical CO<sub>2</sub>.

**Table 2. Solubilities of Ce(tod)<sub>4</sub> and Ce(thd)<sub>4</sub> in Supercritical Carbon Dioxide**

Ce(tod) <sub>4</sub>				Ce(thd) <sub>4</sub>			
P/MPa	ρ/g·L <sup>-1</sup>	10 <sup>3</sup> y	S/g·L <sup>-1</sup>	P/MPa	ρ/g·L <sup>-1</sup>	10 <sup>3</sup> y	S/g·L <sup>-1</sup>
T = 333 K							
14.54	587.6	1.67	19.45	13.31	525.1	0.05	0.49
16.82	662.5	2.99	39.44	15.29	616.9	0.11	1.38
18.60	701.2	4.22	58.92	17.62	681.3	0.23	3.15
21.46	746.4	6.08	90.61	19.68	720.2	0.32	4.63
				22.27	757.0	0.42	6.23
				25.29	790.2	0.50	7.90
				27.88	813.5	0.55	8.92
				30.60	834.4	0.59	9.80
				34.59	860.7	0.62	10.58
T = 323 K							
12.54	616.6	1.63	19.97	11.77	569.8	0.06	0.65
12.82	630.3	2.00	25.05	12.40	609.3	0.08	0.96
14.84	697.8	3.09	42.92	14.18	680.0	0.14	1.86
17.89	756.8	4.63	69.79	16.21	728.1	0.20	2.88
19.99	785.2	6.22	97.53	18.29	762.8	0.25	3.84
24.30	828.8	7.84	129.95	20.31	789.0	0.30	4.66
				23.03	817.4	0.34	5.59
				25.94	842.3	0.38	6.38
				28.56	861.4	0.41	7.05
				31.68	881.2	0.44	7.64
				34.75	898.3	0.45	8.02
T = 313 K							
9.80	611.8	1.53	18.57	10.12	637.7	0.05	0.65
10.43	657.4	1.87	24.44	12.38	729.2	0.10	1.51
12.19	724.7	2.78	40.11	14.42	772.0	0.14	2.19
14.53	773.7	3.95	60.94	16.49	802.4	0.17	2.79
16.93	807.9	4.07	65.56	18.50	825.7	0.20	3.29
				21.44	862.1	0.23	3.85
				24.13	874.1	0.25	4.28
				27.08	893.6	0.26	4.61
				29.87	909.8	0.27	4.87
				32.68	924.4	0.28	5.08
				35.09	935.8	0.29	5.17

Although Fe(tod)<sub>3</sub> is more soluble than Fe(thd)<sub>3</sub>, the solubility difference between these chelates is not as great as that in the case above. It is likely that the smaller ionic radius of Fe<sup>3+</sup> compared to Ce<sup>4+</sup> and Tb<sup>3+</sup> lessens the distinction between tod and thd in terms of metal shielding. Nonetheless, the isobutyl group functions at least as well as the *tert*-butyl group even for first-row transition metal chelates. By contrast, the smaller acac ligand is unable to effectively shield Fe<sup>3+</sup>, and Fe(acac)<sub>3</sub> has very low solubility.

**Terbium Chelates.** To determine whether the terbium chelates were present as the dimer or monomer in supercritical CO<sub>2</sub>, we measured the infrared spectrum of each chelate in CO<sub>2</sub> from 313 to 333 K and 10 to 20 MPa. Tb<sub>2</sub>(tod)<sub>6</sub> or Tb<sub>2</sub>(thd)<sub>6</sub> was loaded into a high-pressure IR cell,<sup>16</sup> and the cell was sealed, heated, and charged with CO<sub>2</sub> to a set pressure. Under all conditions, the characteristic Tb–O–Tb stretch of the dimer was absent from the IR spectra, indicating that only the monomers, Tb(tod)<sub>3</sub> and Tb(thd)<sub>3</sub>, were present in supercritical CO<sub>2</sub>.<sup>9</sup>

**Correlation of Experimental Solubility Data.** The experimental solubility data for the metal chelates were correlated using the empirical model proposed by Chrastil:<sup>7</sup>

$$S = \rho^k \exp(a/T + b) \quad (1)$$

where *S* is the solubility (g/L) of the metal chelate dissolved in supercritical CO<sub>2</sub>, *ρ* is the density (g/L) of pure CO<sub>2</sub> at the experimental temperature and pressure, *k* is the number of CO<sub>2</sub> molecules associated with the metal chelate, *a* = Δ*H*/*R* (where Δ*H* is the sum of the enthalpies of vaporization and solvation), and *b* is a constant. By

**Table 3. Solubilities of Tb(tod)<sub>3</sub> and Tb(thd)<sub>3</sub> in Supercritical Carbon Dioxide**

Tb(tod) <sub>3</sub>				Tb(thd) <sub>3</sub>			
P/MPa	ρ/g·L <sup>-1</sup>	10 <sup>3</sup> y	S/g·L <sup>-1</sup>	P/MPa	ρ/g·L <sup>-1</sup>	10 <sup>3</sup> y	S/g·L <sup>-1</sup>
T = 333 K							
14.06	565.8	0.55	5.01	17.21	671.9	0.28	3.07
14.80	598.3	0.78	7.51	20.73	736.3	0.30	3.52
15.31	617.7	0.88	8.74	23.40	770.3	0.32	4.02
16.76	661.0	1.37	14.61	28.08	815.0	0.34	4.50
17.34	675.0	1.50	16.30	34.97	862.9	0.34	4.73
18.94	707.5	2.12	24.20				
19.58	718.5	2.26	26.26				
20.84	737.9	2.84	33.84				
21.29	744.1	2.79	33.50				
23.67	773.3	3.45	43.11				
T = 323 K							
12.83	630.4	0.53	5.41	12.46	612.7	0.10	1.02
14.65	692.9	1.19	13.34	14.60	691.7	0.15	1.63
14.68	693.7	1.26	14.06	16.53	734.1	0.17	2.01
14.92	699.8	1.08	12.15	18.76	771.2	0.19	2.34
16.57	734.9	1.84	21.80	20.64	792.8	0.20	2.58
16.82	739.3	1.61	19.18	23.71	823.7	0.23	2.99
18.74	769.1	2.52	31.27	26.74	848.4	0.23	3.18
18.96	772.0	2.07	25.77	30.04	871.1	0.24	3.34
20.80	794.6	2.87	36.83	35.23	900.8	0.24	3.48
20.95	796.2	2.41	30.99				
22.57	813.0	3.17	41.68				
23.88	825.2	3.40	45.39				
26.58	847.2	3.72	50.91				
T = 313 K							
12.43	731.0	0.64	7.60	12.46	731.7	0.07	0.88
14.54	774.0	0.87	10.90	15.14	783.6	0.09	1.17
14.98	781.0	0.97	12.20	18.58	826.6	0.11	1.46
16.49	802.4	1.06	13.67	23.39	868.7	0.12	1.70
16.62	804.1	1.15	14.85	30.38	912.5	0.15	2.15
18.77	828.5	1.24	16.52				
20.52	845.3	1.43	19.53				
21.54	854.1	1.40	19.35				
24.83	879.0	1.53	21.74				
25.12	881.0	1.62	23.07				
30.56	913.5	1.64	24.14				
31.84	920.2	1.72	25.48				

**Table 4. Solubilities of Fe(tod)<sub>3</sub> and Fe(thd)<sub>3</sub> in Supercritical Carbon Dioxide**

Fe(tod) <sub>3</sub>				Fe(thd) <sub>3</sub>			
P/MPa	ρ/g·L <sup>-1</sup>	10 <sup>3</sup> y	S/g·L <sup>-1</sup>	P/MPa	ρ/g·L <sup>-1</sup>	10 <sup>3</sup> y	S/g·L <sup>-1</sup>
T = 333 K							
13.11	513.1	1.55	10.97	13.88	556.8	3.91	30.10
14.46	584.2	3.71	29.96	14.22	573.3	4.70	37.29
15.23	614.7	5.02	42.64	15.71	630.9	8.70	76.16
15.90	636.9	6.82	60.19	16.30	648.6	7.88	70.91
16.18	645.2	7.75	69.38	18.48	698.8	10.13	98.40
16.63	657.5	8.60	78.53				
17.74	683.8	12.67	120.80				
T = 323 K							
11.10	512.1	1.39	9.83	12.27	602.1	2.99	24.82
12.46	612.6	4.13	35.00	14.44	687.2	3.72	35.35
12.79	629.0	4.75	41.30	17.25	746.6	4.34	44.79
13.91	671.6	6.20	57.71	20.20	787.7	4.69	51.05
14.47	688.1	8.25	78.75	24.37	829.4	4.82	55.29
16.50	733.6	10.30	105.07	30.67	875.0	5.85	70.85
T = 313 K							
9.06	498.2	1.75	12.03	9.48	575.0	1.64	13.01
9.31	548.2	2.64	19.93	10.40	655.9	2.30	20.83
10.75	673.9	5.48	51.09	12.36	729.0	3.40	34.19
11.28	695.9	6.48	62.50	14.54	774.0	4.24	45.38
12.16	723.8	8.50	85.40	17.30	812.4	4.94	55.55
14.75	777.3	10.32	111.58	20.04	840.9	5.34	62.10
				24.15	874.2	5.60	67.78

performing a multiple linear regression on ln *S* as a function of ln *ρ* and 1/*T*, the coefficients *k*, *a*, and *b* are obtained. These coefficients are listed in Table 6 along with

**Table 5. Solubility of Fe(acac)<sub>3</sub> in Supercritical Carbon Dioxide**

<i>P</i> /MPa	$\rho$ /g·L <sup>-1</sup>	10 <sup>3</sup> <i>y</i>	<i>S</i> /g·L <sup>-1</sup>	<i>P</i> /MPa	$\rho$ /g·L <sup>-1</sup>	10 <sup>3</sup> <i>y</i>	<i>S</i> /g·L <sup>-1</sup>
<i>T</i> = 333 K							
12.76	490.1	0.06	0.24	20.74	736.4	0.26	1.51
14.77	597.5	0.12	0.56	22.82	763.6	0.28	1.74
16.69	659.3	0.17	0.91	24.78	785.0	0.30	1.91
18.74	703.9	0.21	1.21				
<i>T</i> = 323 K							
11.99	585.1	0.07	0.32	22.89	816.1	0.16	1.04
12.68	623.6	0.06	0.31	23.80	824.5	0.15	1.02
13.46	656.4	0.10	0.55	24.92	834.1	0.17	1.14
14.75	695.6	0.09	0.51	24.99	834.7	0.18	1.19
16.31	730.1	0.13	0.74	26.55	847.0	0.17	1.14
16.35	730.8	0.13	0.75	27.13	851.3	0.19	1.29
17.00	742.5	0.11	0.65	29.65	868.6	0.19	1.36
18.33	763.3	0.14	0.84	29.67	868.8	0.18	1.28
18.96	772.1	0.13	0.80	32.36	885.2	0.20	1.39
20.56	791.9	0.15	0.92	33.40	891.0	0.19	1.36
21.25	799.5	0.14	0.92	34.86	898.9	0.20	1.46
<i>T</i> = 313K							
9.82	613.1	0.06	0.28	21.76	856.0	0.22	1.50
10.63	668.0	0.09	0.47	24.55	877.0	0.23	1.59
11.74	711.5	0.12	0.66	24.78	878.7	0.24	1.67
12.46	731.8	0.12	0.72	26.92	892.7	0.24	1.74
13.88	762.4	0.13	0.79	27.54	896.4	0.25	1.79
14.70	776.6	0.15	0.95	29.50	907.8	0.26	1.90
16.01	796.1	0.18	1.14	29.82	909.5	0.25	1.85
16.77	806.1	0.17	1.13	32.36	922.8	0.26	1.96
18.00	820.4	0.19	1.23	32.80	925.0	0.27	1.97
18.92	830.1	0.19	1.28	35.37	937.1	0.27	2.05
19.95	840.1	0.21	1.39				

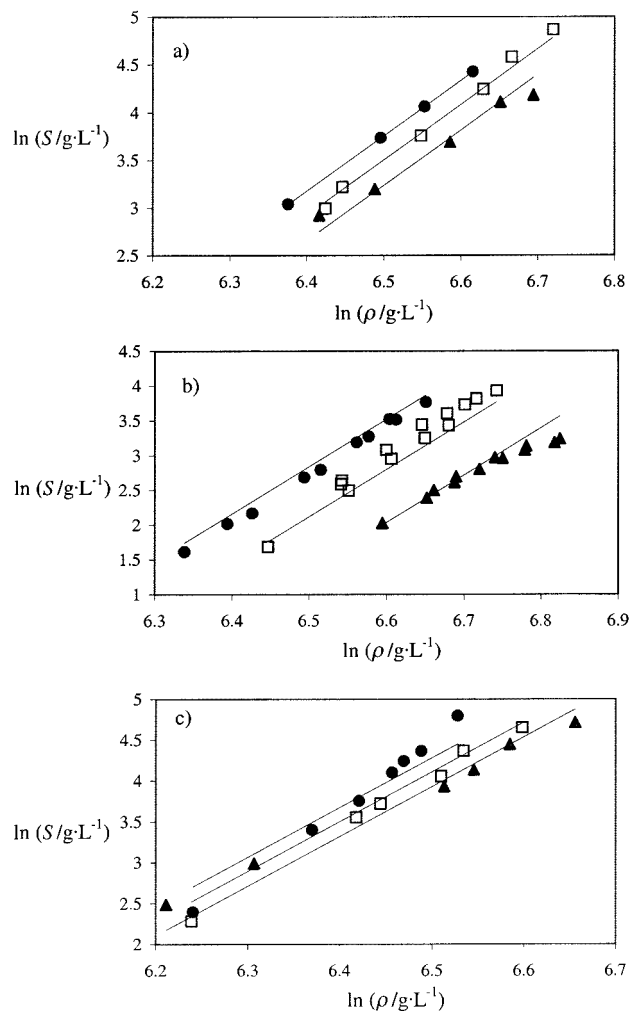
**Table 6. Chrastil Solubility Coefficients ( $\pm 1\sigma$ ) from Eq 1 and Calculated Enthalpies for Metal Chelates Dissolved in Supercritical CO<sub>2</sub>**

compound	<i>k</i>	10 <sup>-1</sup> <i>a</i>	<i>b</i>	% AARD <sup>a</sup>	$\Delta H$ (kJ/mol)
Ce(tod) <sub>4</sub>	5.81 ± 0.24	-272 ± 33	-25.8 ± 0.2	6.5	-22.6
Ce(thd) <sub>4</sub>	5.88 ± 0.15	-588 ± 28	-19.6 ± 1.0	8.7	-48.9
Tb(tod) <sub>3</sub>	6.79 ± 0.35	-773 ± 54	-18.1 ± 1.7	13.3	-64.3
Tb(thd) <sub>3</sub>	3.07 ± 0.20	-643 ± 30	0.3 ± 1.4	6.2	-53.5
Fe(tod) <sub>3</sub>	6.07 ± 0.35	-183 ± 54	-29.7 ± 2.6	13.5	-15.2
Fe(thd) <sub>3</sub>	3.22 ± 0.44	-505 ± 83	-1.6 ± 2.8	20.0	-42.0
Fe(acac) <sub>3</sub>	3.87 ± 0.25	-181 ± 51	-20.1 ± 1.7	18.8	-15.1

$$^a \% \text{ AARD} = 1/N \sum |(S_{\text{exp}} - S_{\text{calc}})/S_{\text{exp}}| \times 100\%$$

$\Delta H$  calculated from *a*. Representative plots of  $\ln S$  versus  $\ln \rho$  are shown for the tod chelates in Figure 3 along with the best-fit line using eq 1.

Smart and co-workers<sup>4</sup> have recently reviewed available metal chelate solubility data and correlated these data to the model of Chrastil in an effort to compile and predict solubilities in supercritical CO<sub>2</sub>. While this correlation is by no means a rigorous method for quantifying intermolecular associations or metal chelate vapor pressures, it does provide a way to compare metal chelate solubilities over a range of densities. For the metal chelates studied, the association number, *k*, ranges from approximately three to seven CO<sub>2</sub> molecules, within the range computed by Smart.<sup>4</sup> Although *k* is expected to depend on density, eq 1 predicts a linear relationship between  $\ln S$  and  $\ln \rho$  with a slope of *k*. Deviations from linearity in fitting eq 1 to the experimental data may arise from potential discrepancies between the actual and calculated densities for the highly soluble chelates. In the Chrastil model,  $\Delta H$  represents the sum of the enthalpy of vaporization and the enthalpy of solvation. Within the series of tod and thd chelates,  $\Delta H$  increases with increasing solubility; for example, Fe(tod)<sub>3</sub>, Ce(tod)<sub>4</sub>, and Tb(tod)<sub>3</sub> have  $\Delta H = -15.2$ ,  $-22.6$ , and  $-64.3$  kJ/mol,

**Figure 3.** Solubility isotherms for (a) Ce(tod)<sub>4</sub>, (b) Tb(tod)<sub>3</sub>, and (c) Fe(tod)<sub>3</sub> in supercritical carbon dioxide at 333 K (●), 323 K (□), and 313 K (▲). Lines represent correlation by eq 1.

respectively. This may simply be the effect of solubility increasing with increased vapor pressure (increased enthalpy of vaporization) although there is not enough thermodynamic data available for these chelates to make definite conclusions.

## Conclusions

The supercritical carbon dioxide solubilities of the  $\beta$ -diketonate complexes Ce(tod)<sub>4</sub>, Ce(thd)<sub>4</sub>, Tb(tod)<sub>3</sub>, Tb(thd)<sub>3</sub>, Fe(tod)<sub>3</sub>, Fe(thd)<sub>3</sub>, and Fe(acac)<sub>3</sub> were measured using near-infrared spectroscopy from 313 to 333 K and 10 to 35 MPa. The resulting solubility isotherms for the metal chelates showed linear behavior versus CO<sub>2</sub> density in a log-log plot. Solubilities of the tod chelates are in all cases higher than those of the thd and acac chelates. The increased flexibility of the isobutyl substituent on tod appears to enhance the shielding of the metal center and may be responsible for the order of magnitude increase in the solubilities of Ce(tod)<sub>4</sub> and Tb(tod)<sub>3</sub> over those of Ce(thd)<sub>4</sub> and Tb(thd)<sub>3</sub>. The Chrastil model correlated the experimental data with average absolute relative deviations of 6.2 to 20.0%.

## Acknowledgment

W.C.A. is grateful to J. N. Webb and T. W. Randolph for the use of their high-pressure infrared cell.

## Literature Cited

- (1) Wai, C. M.; Wang, S. Supercritical Fluid Extraction: Metals as Complexes. *J. Chromatogr., A* **1997**, *785*, 369–383.
- (2) Ashraf-Khorassani, M.; Combs, M. T.; Taylor, L. T. Supercritical Fluid Extraction of Metal Ions and Metal Chelates from Different Environments. *J. Chromatogr., A* **1997**, *774*, 37–49.
- (3) Burford, M. D.; Ozel, M. Z.; Clifford, A. A.; Bartle, K. D.; Lin, Y.; Wai, C. M.; Smart, N. G. Extraction and Recovery of Metals Using a Supercritical Fluid with Chelating Agents. *Analyst* **1999**, *124*, 609–614.
- (4) Smart, N. G.; Carleson, T.; Kast, T.; Clifford, A. A.; Burford, M. D.; Wai, C. M. Solubility of Chelating Agents and Metal-Containing Compounds in Supercritical Fluid Carbon Dioxide. *Talanta* **1997**, *44*, 137–150.
- (5) Darr, J. A.; Poliakoff, M. New Directions in Inorganic and Metal-Organic Coordination Chemistry. *Chem. Rev.* **1999**, *99*, 495–542.
- (6) Rice, J. K.; Niemeyer, E. D.; Bright, F. V. Evidence for Density-Dependent Changes in Solute Molar Absorptivities in Supercritical CO<sub>2</sub>: Impact on Solubility Determination Practices. *Anal. Chem.* **1995**, *67*, 4354–4357.
- (7) Chrastil, J. Solubility of Solids and Liquids in Supercritical Gases. *J. Phys. Chem.* **1982**, *86*, 3016–3021.
- (8) Taylor, B. N.; Kuyatt, C. E. *Guidelines for Evaluating and Expressing the Uncertainty of NIST Measurement Results*; Tech. Note 1297; National Institute of Standards and Technology: Washington, DC, 1994.
- (9) Andersen, W. C. Solubility and Extraction of Cerium(IV), Terbium(III), and Iron(III)  $\beta$ -Diketonates in Supercritical Carbon Dioxide. Ph.D. Thesis, University of Colorado, Boulder, 2000.
- (10) Wenzel, T. J.; Williams, E. J.; Haltiwanger, R. C.; Sievers, R. E. Studies of Metal Chelates with the Novel Ligand 2,2,7-Trimethyl-3,5-Octanedione. *Polyhedron* **1985**, *4*, 369–378.
- (11) Inomata, H.; Yagi, Y.; Saito, M.; Saito, S. Density Dependence of the Molar Absorption Coefficient—Application of the Beer–Lambert Law to Supercritical CO<sub>2</sub>–Naphthalene Mixture. *J. Supercrit. Fluids* **1993**, *6*, 237–240.
- (12) Swaid, I.; Nickel, D.; Schneider, G. M. NIR–Spectroscopic Investigations on Phase Behaviour of Low-Volatile Organic Substances in Supercritical Carbon Dioxide. *Fluid Phase Equilib.* **1985**, *21*, 95–112.
- (13) Lagalante, A. F. The Measurement, Modeling, and Applications of Metal  $\beta$ -Diketonate Complexes Dissolved in Supercritical Carbon Dioxide. Ph.D. Thesis, University of Colorado, Boulder, 1995.
- (14) Lagalante, A. F.; Hansen, B. N.; Bruno, T. J.; Sievers, R. E. Solubilities of Copper(II) and Chromium(III)  $\beta$ -Diketonates in Supercritical Carbon Dioxide. *Inorg. Chem.* **1995**, *34*, 5781–5785.
- (15) Span, R.; Wagner, W. A New Equation of State for Carbon Dioxide Covering the Fluid Region from the Triple-Point Temperature to 1100 K at Pressures up to 800 MPa. *J. Phys. Chem. Ref. Data* **1996**, *25*, 1509–1596.
- (16) Designed by J. N. Webb and T. W. Randolph. Department of Chemical Engineering, University of Colorado, Boulder, CO 80309-0424.

Received for review August 4, 2000. Accepted December 20, 2000. W.C.A. is grateful to the U.S. EPA and CIRES Graduate Fellowship Programs for financial support.

JE000257C